Input gain control confers robust combinatorial odor coding in naturalistic environments

Nirag Kadakia[1,2] and Thierry Emonet[2,3]

[1] Swartz Fellow of Theoretical Neuroscience
[2] Department of Molecular, Cellular, and Developmental Biology, Yale University, New Haven, CT 06511, USA
[3] Department of Physics, Yale University, New Haven, CT 06511, USA

August 28, 2018

Animals identify and discriminate odors using olfactory receptors (Ors) expressed in olfactory receptor neurons (ORNs) [1, 2]. In both insects and vertebrates, distinct ORNs, which typically express a single Or, respond broadly to many distinct volatile odorants [3, 4, 5, 6, 7, 8]. Likewise, any given odorant may incite strong responses in a number of ORNs. ORN tuning curves are therefore broad and overlapping, implying that odors are encoded combinatorially – by the particular combination of responses they elicit in the ORN repertoire, patterns which are eventually decoded downstream into behavioral response [9].

Odor signals in nature are uniquely complex in composition, space, and time, and like other sensory modalities, olfactory systems must tune their response to the character of input stimuli [10, 11, 12, 13, 14]. Various features of natural odor signals are power-law distributed, producing whiffs of widely varying duration and intensity [12]. Sensitivity to low concentrations could thus lead to saturation at high intensities, confounding combinatorial representations of odor identity. Further, ethologically-relevant odors are often mixed together with nuisance odors; due to the non-specificity of ORN response, distinct odors could simultaneously activate overlapping ORN subsets, preventing accurate disambiguation [15].

What invariances and adaptive mechanisms might help preserve combinatorial odor representations in natural environments? In *Drosophila* larvae, dose responses of 324 OR-odorant combinations obey a single activation function shape, with similar Hill coefficients but different activation thresholds, which are distributed as a power law [16]. *Drosophila* ORNs also exhibit a large degree of similarity in their temporal integration of fluctuating stimuli. While for some Or-odor combinations, ORN response can exhibit large differences, such as super-sustained responses [17], deconvolution of stimulus dynamics from neuron responses produces stereotyped filters that differ little among ORNs [18].

Beyond these invariances are adaptive mechanisms which can preserve odor representations amid environmental changes. In *Drosophila*, antennal lobe glomeruli receiving connections from ORNs send mutually inhibitory connections, effectively normalizing incoming ORN signals before they are projected to the lateral horn and mushroom body [19]. In the mushroom body, inhibition from giant interneuron upon Kenyon cells further acts to suppress patterns of activity elicited by these odors [20]. Further, upstream of these connectivity-mediated mechanisms, individual ORNs themselves adapt in time an apparently universal way: ORN gain varies inversely with mean odor concentration according to Weber's Law of psychophysics [21], while maintaining response time independent of odor intensity [14, 22, 23]. Weber's Law has been observed in several OR-odorant combinations, and is traced to feedback mechanisms operating at the level of odor transduction, upstream of ORN firing machinery [14]. This points to a mechanistic origin involving modification of phosphorlyation sites on the universal *Drosophila* co-receptor Orco. Other phosphorylation sites on Orco have been implicated in desensitization to odors over longer timescales as well [24, 25].

While in a single channel system such as *E. coli*, adaptive feedback via Weber's Law is known to robustly maintain sensitivity in response to mean concentration changes, the implications for a multiple-channel system – which combines information from several sensors with overlapping receptive fields – is less straightforward. Here we combine a biophysical model of universal ORN adaptive response and neural firing with various sparse signal decoding frameworks to explore whether and how ORN adaptation maintains accurate combinatorial coding of odor signals that span varying degrees of intensity, molecular complexity, and temporal structure. We find that front-end gain modulation helps preserve coding capacity within the non-specifically sensing ORN repertoire, and maintains abstract representations of odor identity across different intensities. As such, this adaptive mechanism promotes the accurate discrimination of weak odor signals from strong backgrounds of varying molecular complexity, both in static odor environments and in fluctuating, naturalistic ones. We also investigate the predictions of our model for the *primacy coding* hypothesis – that odors are encoded entirely by the subset of a few earliest responding ORNs [26, 27]. Our results agree with primacy coding when odor signals are sufficiently simple, though signals composed of more molecular constituents require the recruitment of the full ORN repertoire. Finally, we show that front-end adaptation acts in concert with divisive normalization in the antennal lobe to maintain the invariance of activity patterns in the mushroom body. Together, our results suggest that despite the broad overlap of ORN tuning curves, a universal mechanism of front-end adaptation may play a vital role in preserving representations of odor

identity in naturalistic odor landscapes.

Results

a Model of ORN sensing repertoire

Odor identification consists of encoding in the sensing periphery followed by decoding in higher-level processing centers of the olfactory circuit. We first examine how front-end adaptation can maintain odor encoding capacity, by drawing upon a model of odor-to-ORN firing recently shown to reproduce experimental findings: Weber-Fechner scaling, signal transduction kinetics, and firing rate dynamics of individual *Drosophila* ORNs to fluctuating stimuli [14]. Here we generalize this model to a repertoire of $M = 50$ ORN types. ORNs house olfactory receptor complexes C_a, $a = 1, ..., M$, each consisting of an ORN-specific OR and the universally-expressed olfactory co-receptor Orco, which mediates odor transduction through dendritic localization of and heteromerization with ORs (Fig. 1a). These odorant-response functional units interact with odor mixtures, each of which is composed of some combination of N odorant molecules with time-dependent concentrations $s_i(t)$, $i = 1, ..., N$ (Fig. 1b). We choose $N = 150$, as this number is sufficiently larger than the size of the sensing repertoire M. Functionally, C_a forms a non-selective cation channel whose current is mediated by the strength and nature of bound ligands. We thus model a given complex as stochastically switching between active (channels open) and inactive states, while also being bound or unbound with odorant i. The active conformation binds odorant i with higher affinity than the inactive conformation, resulting in distinct dissociation constants, K^*_{ia} and K_{ia}, respectively. In steady state, the active fraction A_a of Or/Orco complexes in ORN a can be solved for as (see Methods):

$$\begin{aligned} A_a(t) &= \left(1 + e^{\epsilon_a(t)}\right)^{-1} \\ \epsilon_a(t) &= \epsilon_{a,\mathrm{act}}(t) + \epsilon_{a,\mathrm{ligand}}(t) \\ \epsilon_{a,\mathrm{ligand}}(t) &= \frac{1 + \sum_i^N s_i(t)/K_{ai}}{1 + \sum_i^N s_i(t)/K^*_{ai}}, \end{aligned} \tag{1}$$

where $\epsilon_{a,\mathrm{act}}(t)$ is the free energy cost of C_a activation.

Inward currents elicited by activation of the Or/Orco receptor complexes then incite firing activity in ORNs. Following [14], we model the Or/Orco-to-ORN transformation with a temporal filter followed by rectifying nonlinearity f (see Methods):

$$r_a(t) = f\left(\int h(\tau - t) A_a(t) d\tau\right). \tag{2}$$

At the single ORN level, this nonlinear-linear-nonlinear framework (Or/Orco activation → temporal filter → nonlinear rectifier) reproduces signal transduction kinetics, notably the temporal slowdown of the local field potential upon adaptation.

Here $\epsilon_a(t)$ represents the free energy change due to modifications of the Or/Orco complexes by adaptation. Opening of the channels causes an inward current that eventually results in a negative feedback onto $A(t)$. This is modeled minimally by:

$$\frac{d\epsilon_a(t)}{dt} = \frac{A_{a0} - A_a(t)}{\tau_a} \tag{3}$$

within the finite range $\epsilon_{\mathrm{L},a} < \epsilon_a(t) < \epsilon_{\mathrm{H},a}$. It has been shown that when properly deconvolved from the stimulus dynamics, the shape of temporal kernels in adult *Drosophila* ORNs is largely odor-independent, though may differ by brief (∼10 ms) odor-dependent delays [18]. Accordingly, we model $h(t)$ by an ORN- and odor-independent double-exponential function, with parameters matched to experiment [18]. We assume that the lower cutoffs $\epsilon_{\mathrm{L},a}$ are receptor-dependent and choose them from a normal distribution. This variability ensures that ORNs are activated above quiescence (around 5 Hz) at distinct stimulus levels [14].

Diversity among maximal odor-ORN response arises from the distribution of chemical affinities, encapsulated in K^*_{ai}. We choose these from a power law distribution ($\alpha = 0.35$), as was recently found across ORN-odor pairs in *Drosophila* larvae. To mimic the presence of private odors relevant to innate responses, we manually add a high responder ($K^*_{ai} \sim$ small) to a handful of ORNs; the addition of these private odors did not affect the general findings. Together, the power-law distributed K^*_{ai}, receptor-dependent $\epsilon_{\mathrm{L},a}$, and invariance in temporal filters, when incorporated into the steady-state model responses Eq. 1, produce tuning curves mimicking the maximal *Drosophila* ORN responses to many individual odorants [6] (Fig. 1c-1e).

b Concentration-invariant preservation of information capacity and odor identity

To investigate the dependence of encoding capacity on odor concentration, we calculate the mutual information (MI) between odor signals $\mathbf{s}$ and responses

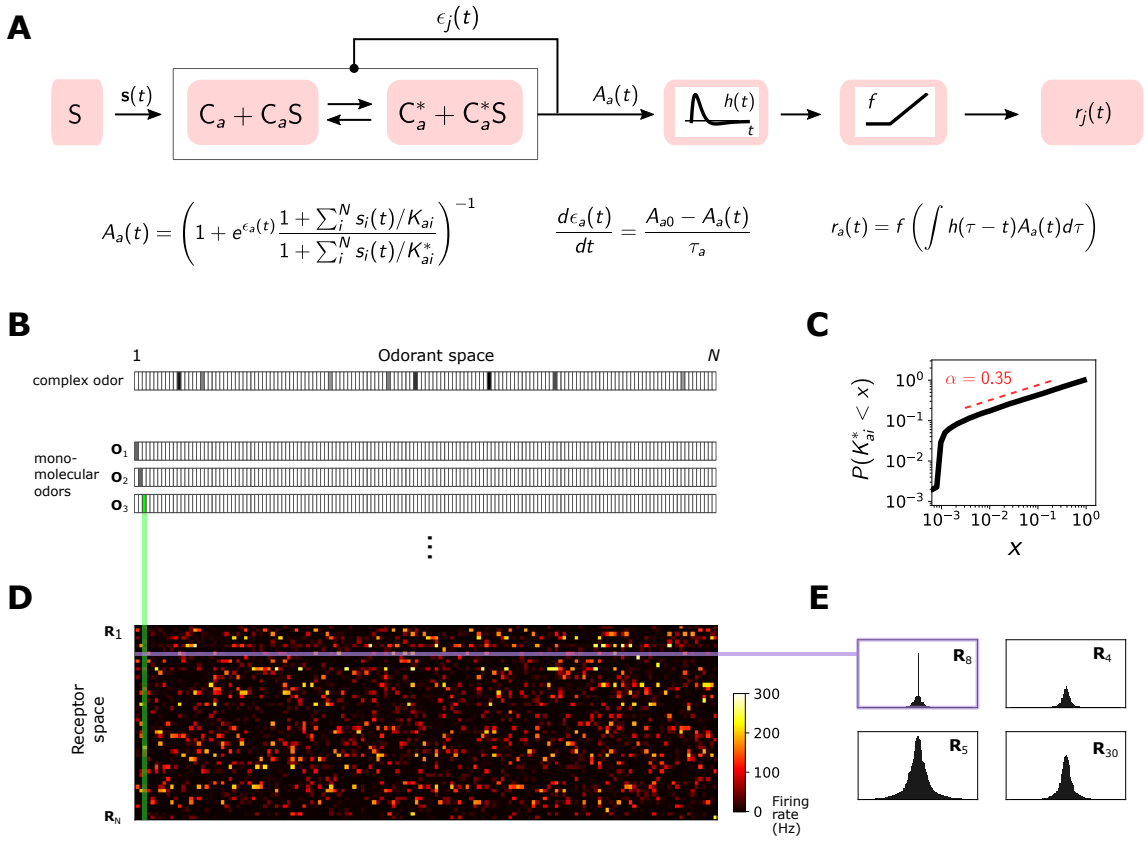

Figure 1: **A** Odor binding model. Or/Orco complexes C_a bind odorant molecules s_i comprising stimuli S. These complexes can stochastically switch between inactive and active states, where the steady-state active fraction is determined by the complex free energy $\epsilon_a(t)$. The activity feeds back on to the free energies with timescale τ_a to pull the activity to a baseline level A_{a0}. ORN firing rates $r_a(t)$ are generated by passing $A_a(t)$ through a linear temporal filter $h(t)$ and a nonlinear thresholding function$f$. **B** Odor mixtures are represented by real-valued N-dimensional vectors $\mathbf{s}$, whose components s_i are the concentrations of the individual molecular constituents of $\mathbf{s}$. **C** Following (), active binding constants are distributed as a power-law with coefficient $\alpha = 0.35$ **D** The maximal firing response of 50 ORNs to the 150-possible monomolecular odors $\mathbf{s} = s_i$, for the power-law K_{ai}^* distribution in C. **E** Representative ORN tuning curves, generated by ordering the responses within a single row of the response matrix in D. A diversity of response, mimicking that of [6], arises from both the distribution of odorant binding constants K_{ai}^* and the distribution of receptor free energies ϵ_a.

$\mathbf{a}$ in two sensing systems, one with ORN adaptive feedback (via Eq. 3) and one without. We consider a simple situation, in which a step of odor A, $\mathbf{s}_A$, turns on at time t_1, persists for some time, and then odor B, $\mathbf{s}_B$ (a distinct identity) turns on at some later time t_2. For simplicity, we assume that both odors have the same intensity s_0 and calculate the MI between the ORN responses $\mathbf{r}_a$ and signals $\mathbf{s}_A + \mathbf{s}_B$ at various times after t_1, as a function of s_0. In the non-adaptive case, the mutual information peaks around the region of maximum sensitivity ($\sim 10^2$ a.u.) after t_1. ORNs are firing at an elevated rate, however, more susceptible to saturation with further odor onsets. Thus, following t_2, the maximum shifts leftward as odors of high intensities have saturated the system and cannot pass any more information.

The adaptive system mimics the non-adaptive system at t_1, before adaptation has kicked in. As the activity feeds back onto ϵ_a, the response to higher concentrations passes through the regime of high sensitivity, and the MI peak shifts rightward. Over time, the responses for all signals have reached the baseline firing rate, and the mutual information is mostly eliminated since the firing rate is independent of odor

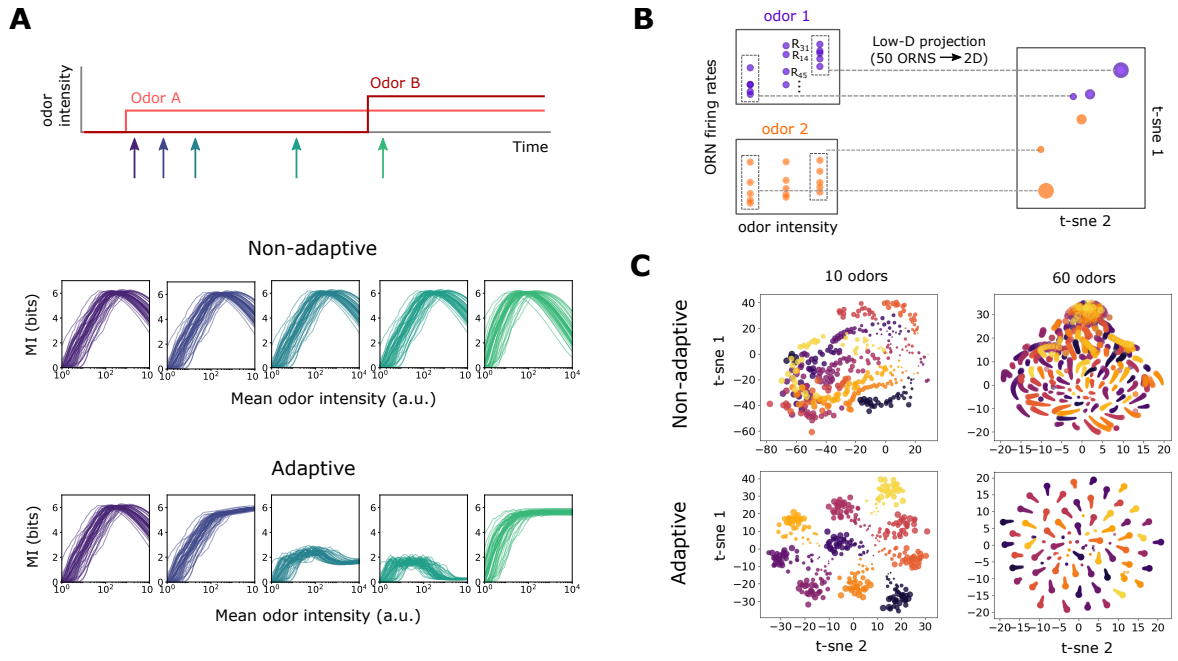

Figure 2: Front-end adaptation maintains information capacity and representations of odor identity across changes in intensity. **A** Evolution of mutual information (MI) between odor signals and ORN response, as a function of relative odor concentration. Odor A arrives at t_1 and Odor B (of the same concentration) arrives at t_2, where $t_2 - t_1 \gg \tau_A$. MI is plotted for both an unadaptive and adaptive system at times of order of τ_A) following t_1(purple; purple-blue), right before t_2(blue-green), and shortly after t_2 (green). **B** To investigate abstract representations of odor identity in the ORN response, ORN responses are projected from 50 dimensions to 2 dimensions, using nonlinear dimensionality reduction. In the 2D space, distinct odors are plotted as points of distinct colors, and point size represents odor intensity. **C** In the adaptive system, responses cluster by identity more apparently for an adaptive system (bottom row), than a non-adaptive system (top row), shown here for 10 and 60 sparse odor identities for several concentrations each.

identity. However, having now adjusted its regime of maximum sensitivity to the presence of odor A, the system can respond appropriately to odor B: the MI at t_2 is nearly 6 bits across 3 decades of concentration, in sharp contrast to the non-adaptive case. These results suggest that in this multi-channel compressive system, a simple mechanism of universal integral feedback can help maintain sensitivity in changing environments.

We thus expect that this preservation of information capacity can help the olfactory circuit maintain abstract representations of odor identity across changes in intensity. To examine such representations, we project the ORN response repertoire to a lower dimensional space using t-distributed stochastic neighbor embedding (t-SNE), a nonlinear, local dimensionality reduction technique. Here, data points are 50-dimensional vectors representing the collective ORN firing response to a given odor of a given intensity. Each of these data points is then reduced by t-SNE to two dimensions. Testing this both for a smaller odor repertoire (10 odor identities) and a larger one (60 identities), we find that odors separate by identity in the adaptive system, while in the unadaptive system, representations mix among their identity and concentration. Together, these results suggest that at the level of ORN response, front-end adaptation helps maintain representations of odor identity across changes in their concentration.

c Front-end adaptation promotes odor decoding and discrimination accuracy amid potential confounds

Next, we ask how well these abstract representations of odor identity can be decoded from the repertoire of ORN response. One potentially complicating factor in signal reconstruction is the disparity between mea-

surement dimension and stimulus dimension: while *Drosophila* only express 60 olfactory receptor genes, the space of aromatic odorants is 10^3 or more, suggesting that information must be passed via combinatorial

. However, many naturally-occurring odors are comprised of only a small subset of these volatile compounds – they are sparse in the space of odorants [28]. This is suggestive as mathematical results in compressed sensing guarantee the reconstruction of these sparse signals, assuming a sufficiently random response [29, 30, 31]. We emphasize that while at this stage of the analysis we use a compressed sensing framework to decode these sparse signals, there is no evidence that this algorithm is being implemented in the *Drosophila* olfactory circuit. Later, we show that similar conclusions follow for odor categorization via binary and multi-class classification.

To incorporate the linear framework of compressed sensing into our nonlinear encoding model, we treat the odor encoding process exactly, while approximating the decoding to first order. Specifically, we represent the nonzero components s_i of a sparse odor mixture as $s_i = s_0 + \Delta s_i$, where s_0 is the center of the linearization. The target of the decoding process are the 'excess' odor signal components Δs_i, which are determined by enforcing signal sparsity and the measured ORN responses through constrained optimization. The cost function to be optimized and the linear constraints are (see Methods):

$$\hat{\mathbf{s}} = \arg\min \sum |s_i| \tag{4}$$

$$\Delta r_a = f\left(\int h(\tau - t)\frac{dA_a}{ds_i}d\tau\right)\Big|_{s_0} \Delta s_i \tag{5}$$

To assess the decoding performance, we denote an odor signal as accurately decoded if (i) the sparse odorant components are all estimated to within 25% of their correct value and (ii) the components absent in the original signal "zero" components) are all estimated as less than 10% of the mean excess concentration, $\hat{s}_i \leq \langle \Delta s_j \rangle$.

We apply this scheme to the ORN system described above, consisting of 50 Or/Orco complexes interacting with a 150-dimensional odorant space. We assume that number of nonzero odorants comprising the odor, K, is small. Note, however, that this still allows for a huge number of distinct odors, e.g. nearly 1 billion for $K = 7$. In the absence of ORN adaptation, signals are still correctly inferred in a particular regime of mean odor concentration (Fig. 3b), corresponding to that of higher coding capacity in Fig. 2a. Elsewhere, decoding accuracy is low. Conversely, enforcing Weber-Fechner scaling within the thresholds $\epsilon_{\mathrm{L},a}$ and $\epsilon_{\mathrm{H},a}$, coding fidelity is maintained over a several-fold change in odor intensity (Fig. 3b).

In natural odor environments, accurate olfactory sensing relies on the ability to discriminate multiple odors, which may differ in chemical makeup and intensity. Even if adaptation could preserve decoding accuracy of a single odor amid intensity changes, it is conceivable that a system which adapts to average concentrations alone may well fail for multiple odors of widely differing concentrations. Accordingly, we next consider two sparse odors, which we call the "foreground" and "background", and ask how well foreground odors can be decoded in the presence of backgrounds of a given intensity and molecularly complexity. In the unadaptive system, decoding accuracy in the regime of maximum sensitivity is maintained if the background concentration is low enough, but is compromised as concentration increases (Fig. 3c). For higher background concentrations, molecular complexity also has a more damaging effect on decoding accuracy. Finally, for sufficiently strong and complex background odors, the foreground is virtually undetectable (top right plot in Fig. 3c). The adaptive system is substantially more robust to backgrounds (Fig. 3d), although the minimum detectable concentration increases with background intensity. Taken together, these results indicate a universal mechanism of adaptive feedback operating on the activity of Or/Orco complexes promotes odor identification amid potential confounds in both identity and intensity.

d Odor decoding in fluctuating odor environments

So far, we have assumed that odor signals are static in time, and that adaptation from the neural circuitry feeds back onto the receptor sensitivity instantly and perfectly. But realistic odor environments are highly intermittent and widely fluctuating, with odor concentrations that can span several orders [12]. Further, metabolic constraints can limit adaptation speed and accuracy [32]. To account for temporal aspects in both the odor environment and sensing periphery, we now assume that changes in Or/Orco receptor complex activity feed back onto receptor activation energies as in Eq. 3 with a timescale $\tau_A = 250$ ms. For simplicity, we assume that while the sensory response modulates in time, the decoding process itself is instantaneous. (mention behavioral latency times). We

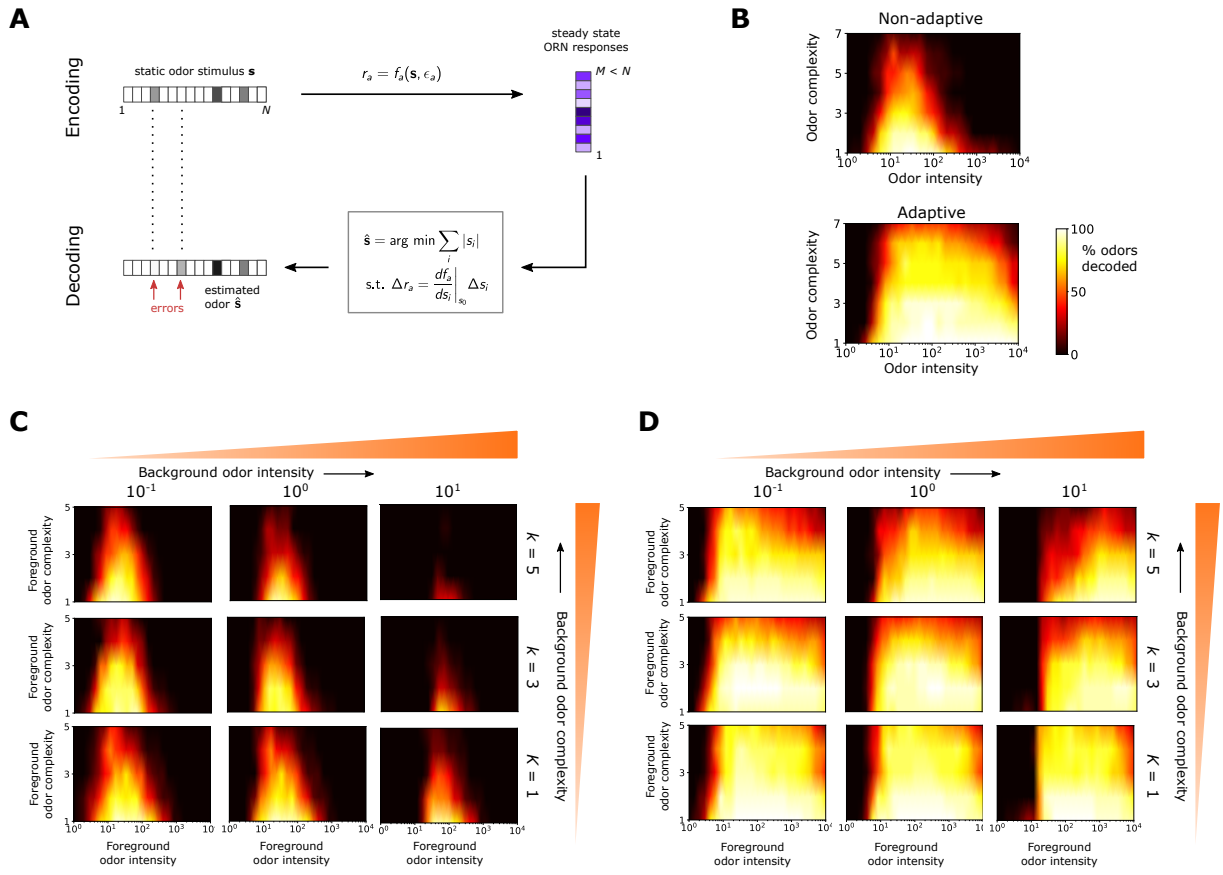

Figure 3: Front-end adaptation promotes accurate sparse odor decoding across concentration changes. **A** Odor stimuli produce ORN response repertoire via odor-binding and activation and firing machinery, as described by Eqs. 1-2. Odors are then decoded using compressed sensing by linearizing around a background s_0 and minimizing the constrained L_1 norm of the odor signal. Odors are assumed sparse, exhibiting K nonzero components, $K \ll N$. **B** Decoding accuracy as a function of odor concentration (a.u.) and odor complexity K, for the non-adaptive and adaptive system respectively. **C** Decoding accuracy of foreground odors in the presence of background odors. Individual plots the decoding accuracy of the foreground as a function of its intensity and complexity, for the given background odor conditions; the intensity of the background odor increases by column and its complexity by row. **D** Same as (C), for the adaptive system.

also mimic a finite length of short-term memory, such that only changes in detected odor signal are remembered, and only for up to τ_F seconds in the past. If the signal is static, it will be decoded optimally between $\sim \tau_A$ and $\sim \tau_F$. For fluctuating environments, we expect that τ_F a few times as large as τ_A should be sufficient in detecting of whiffs of novel odors amid slowly fluctuating or static backgrounds.

We first consider the simple case of step stimuli. For shallow steps, odors are rapidly decoded, though slightly more quickly for smaller τ_A. This is attributed the recruitment of a sufficient number of ORNs beneath the point of response saturation, such that response adaptation has little effect. For larger steps, decoding accuracy improves gradually as the system adapts at its characteristic timescale. In all cases, the accuracy drops to zero after the forgetting time τ_F (here set to $4\tau_A$).

We next considered a naturalistic plume, using a recorded time trace from a photo-ionization detector placed downwind of an odor source, Fig.(X) (see Methods). The time trace was scaled linearly to

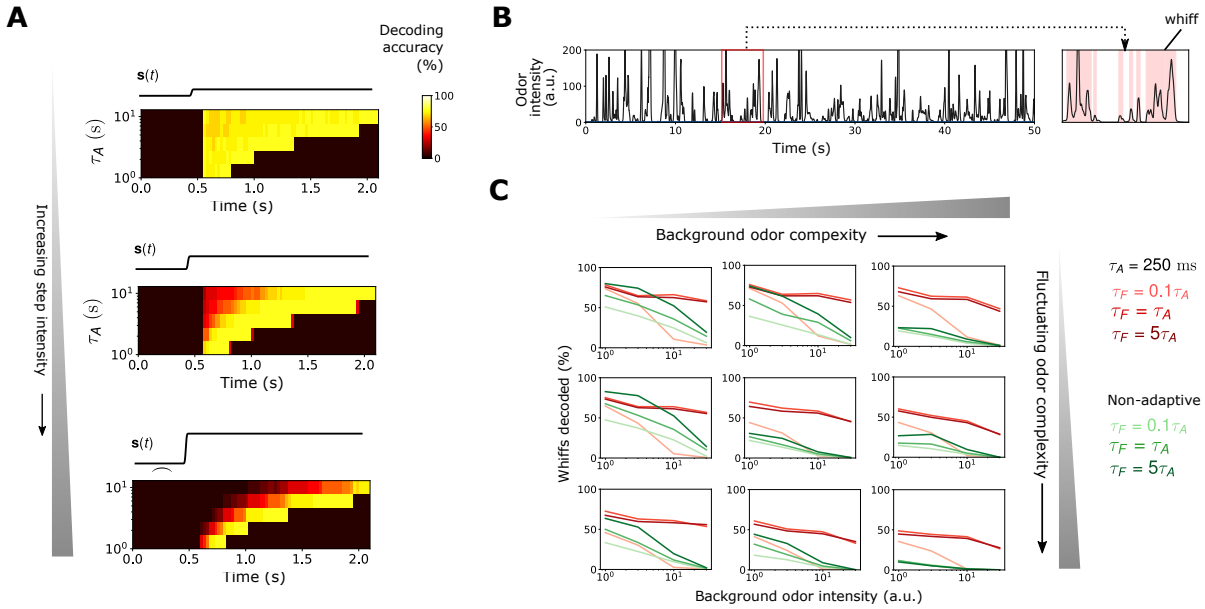

Figure 4: Universal ORN adaptation operating at measured timescales aids the identification of individual odor whiffs in naturalistic odor environments. **A** Odor decoding accuracy before and after the onset of a step stimulus. Each plot shows the decoding accuracy in time for increasing adaptation time τ_A; the plots are arranged in order of increasing step stimulus strength. **B** Naturalistic odor signal measured with photo-ionization detector downwind of a source of apple cider vinegar. Whiffs are defined as contiguous regions in which the intensity is above 10 a.u. **C** Individual plots: whiff decoding accuracy as a function of background odor intensity; $\tau_A = 250$ ms in red and non-adaptive in green, light to dark for increasing τ_F. Rows: increasing complexity of the fluctuating odor; columns: increasing complexity of background odor.

values applicable to our model framework (in arbitrary units), and we verified that the plume statistics agree with theoretical predictions (supp fig). The signal is composed of an series of intermittent "whiffs," defined as contiguous regions at which the concentration is above a given value (see Methods). This signal serves as the intensity of the odor, to which we randomly assign a sparse identity from the N-dimensional odor space, as above. To investigate discrimination on potentially confounding backgrounds, we add to this signal a static background odor of varying intensities and complexities, and calculate the percentage of correctly decoded odor whiffs (see Methods).

For odors

e Relationship to primacy coding hypothesis

An intriguing hypothesis that has emerged from recent experiments in vertebrates – "primacy coding" – suggests that odor identity is encoded entirely by the subset (but not temporal order) of earliest responding glomeruli (Fig. 5a). By optogenetically masking odors at a certain point beyond the odor onset, it is found that behavioral response is completely preserved provided the mask latency sufficiently long. Glomeruli active before mask onset are those that encode the odor identity (the primacy set), while those that activate after add no further information. Importantly, if identical across odor intensities, these primacy sets would form a concentration-invariant representation of odor identity.

In our framework, odors are decoded via information passed simultaneously from all 50 ORNs. However some of this information may be redundant, whereby a set of earliest active ORNs are sufficient for odor recognition; if so, our theory would generate predictions in agreement with primacy coding. To test this, we consider a steep sigmoidal stimulus with half-max slope of $1/50$ ms^{-1}, as in Fig. 5a. We calculate the decoding accuracy as a function of time, and plot in Fig. 5b the accuracy as a function of number

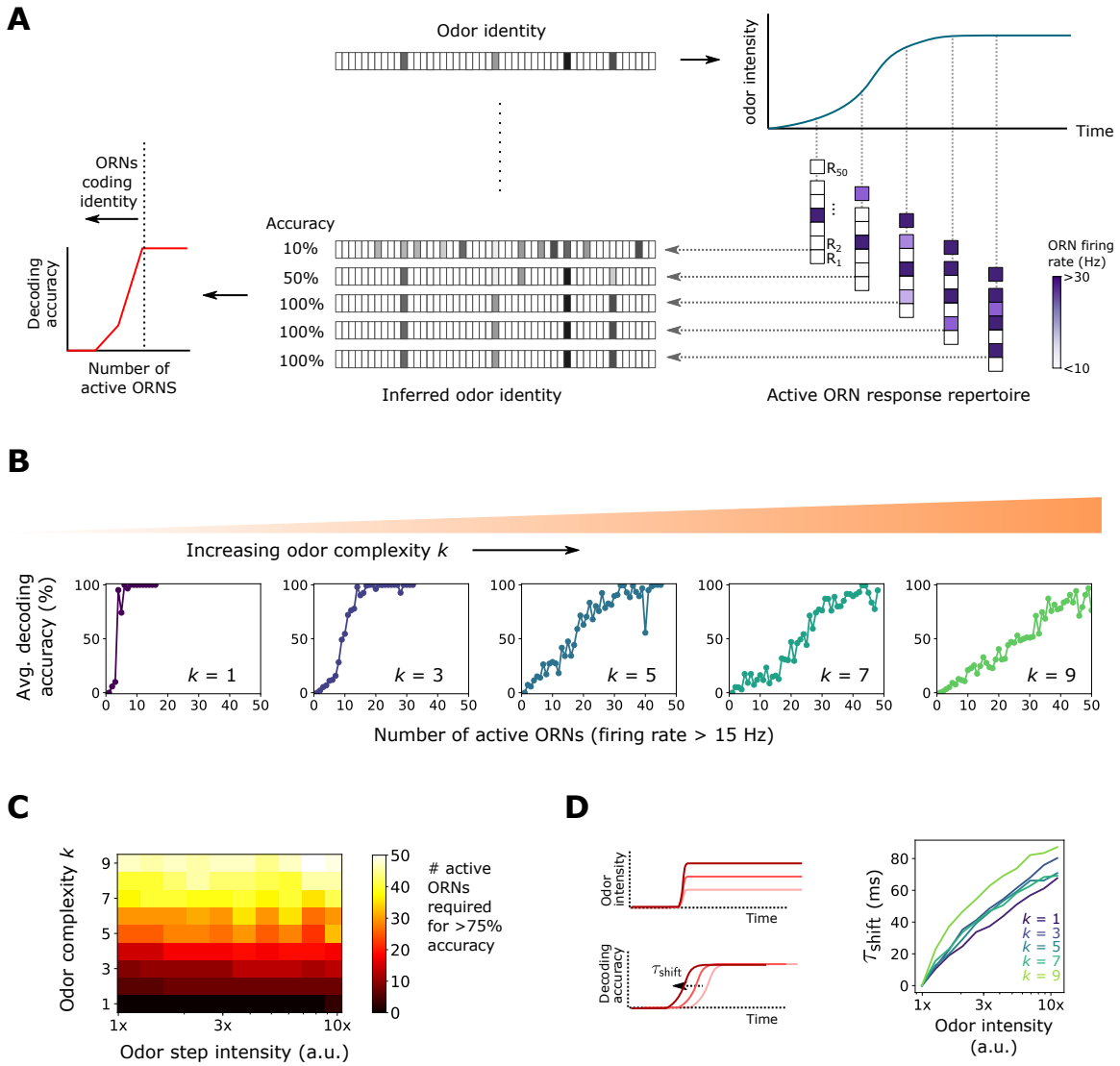

Figure 5: TODO

of active ORNs, which increases monotonically as the signal rises (Fig. 5a). To illustrate how the recruitment of ORNs incrementally improves odor signal recognition, we allow for partial accuracy by calculating the percentage of correctly decoded individual odor components.

For sufficiently simple odors, our results are indeed in accordance with primacy coding: the set of earliest responding neurons fully account for the odor identity ($K = 1, 3, 5$ plots in Fig. 5b). Though all ORNs eventually activate as the stimulus increases, the latter responders confer no further information in odor recognition. As expected, the active ORN subset comprising the primacy set is distinct for each odor, Show that recruited ORNs are all distinct. We do find, however, that for more complex odor mixtures, the full ORN repertoire must be active for accurate decoding ($K = 7, 9$ plots in Fig. 5b), a result that holds across odor odor concentrations Fig. 5c). In this regime, our framework is somewhat at odds

with primacy coding, since a primacy set consisting of the full ORN repertoire would encode only a single odor. Our framework is capable of decoding the odor for a maximal primacy set since it utilizes not just the identity of the active ORNs, but also their individual firing responses. Say more here

The primacy coding hypotheses also predicts that for stronger stimuli, behavioral responses shift earlier in time, since the primacy set is activated quicker. We calculate the time shift for increasingly higher intensities. For all mixture complexities, this shift rises monotonically with odor intensity over a decade of concentrations. The timescale is on the same order as those measured (18 ms measured; here 60 ms), though the model organisms are different, so this may not be particularly meaningful. Together, these results suggest that front-end adaptation, in concert with the compressed sensing paradigm, are in agreement with the predictions of the primacy coding hypotheses. Our framework also provides the testable prediction that primacy coding may be limited in response to more complex odor mixtures.

f Cooperative effects of ORN adaptation and downstream normalization

Lateral inhibition among antennal lobe glomeruli normalizes ORN responses prior to their projections to the mushroom body. This inhibition has been shown to obey a type of divisive gain control, normalizing each input by the sum of the activity. To what extent does Weber Law adaptation in the olfactory periphery act in tandem with (or confound) this downstream normalization to maintain odor representations? To investigate this, we extended our ORN encoding model by adding uniglomerular connections from ORNs to the antennal lobe, followed by sparse, divergent connections to 2500 Kenyon cells (KCs) in the mushroom body (Fig. 6a). Following [], divisive normalization was modeled via []:

$$a(t) = ... \tag{6}$$

We then quantified decoding accuracy by training and testing a linear classifier on the KC activity output of many sparse odors of distinct intensity and identity, each randomly categorized as appetitive or aversive. Odor signals of the same identity but differing intensity were assigned the same valence (Fig. 6a) (although, see..). We trained the classifier on p sparse odor identities at intensities chosen randomly over 4 orders of magnitude, then tested the classifier accuracy on the same odor identities but of differing concentrations.

In general, classification accuracy degrades to chance level when the number of distinct odor identities p is very high; however, this is mitigated by the presence of divisive normalization alone (e.g. performance increases from $\sim 65\%$ to 75% for $p = 500$) (Fig. 6b), and even moreso by ORN adaptation alone (to 85%). Further, with both AL normalization and ORN adaptation, accuracy remains above 90% for p up to 500, suggesting that these distinct adaptive transformations may act jointly in preserving representations of odor identity. As expected, performance improves without adaptive mechanisms when the intensity range is narrower, and these gains are mostly erased (Fig. 6c). Interestingly, if we instead train the classifier to distinguish odors by their distinct identity using multiclass classification (Fig. 6a), we find that the benefits conferred by divisive normalization do not appear until p is substantial, with accuracy below 65% for $p \sim 50$ (Fig. 6d). On the other hand, with ORN adaptation accuracy remains above 85% for p as high as 1000. Together, these results suggest that front-end adaptation plays a key role in maintaining odor identity representations, before they are further normalized and diverged in downstream processing. In some categorization tasks, subsequent normalization can further preserve these representations.

Discussion

This whole section is old and needs to be updated.

Drawing on recent evidence for the existence of the Weber-Fechner law in in *Drosophila* olfactory receptor neurons [22, 23, 14], we propose a theoretical framework for the adaptive encoding and decoding of complex, dynamic odor environments. We argue that this adaptive mechanism, when incorporated into a combinatorial coding strategy, is central to the accurate identification and discrimination of rapidly fluctuating, potentially conflicting odor signals. Our framework relies on two steps of odor encoding and decoding, respectively: (i) a nonlinear, stochastic model of odor-receptor binding and subsequent receptor activity, and ii) reconstruction of the signal via compressed decoding of the neural response. In this framework, input gain control following the Weber-Fechner Law is enforced by appropriate scaling of the free energy of Or/Orco complex activation with the odor signal mean.

The encoding model is a generalization of the clas-

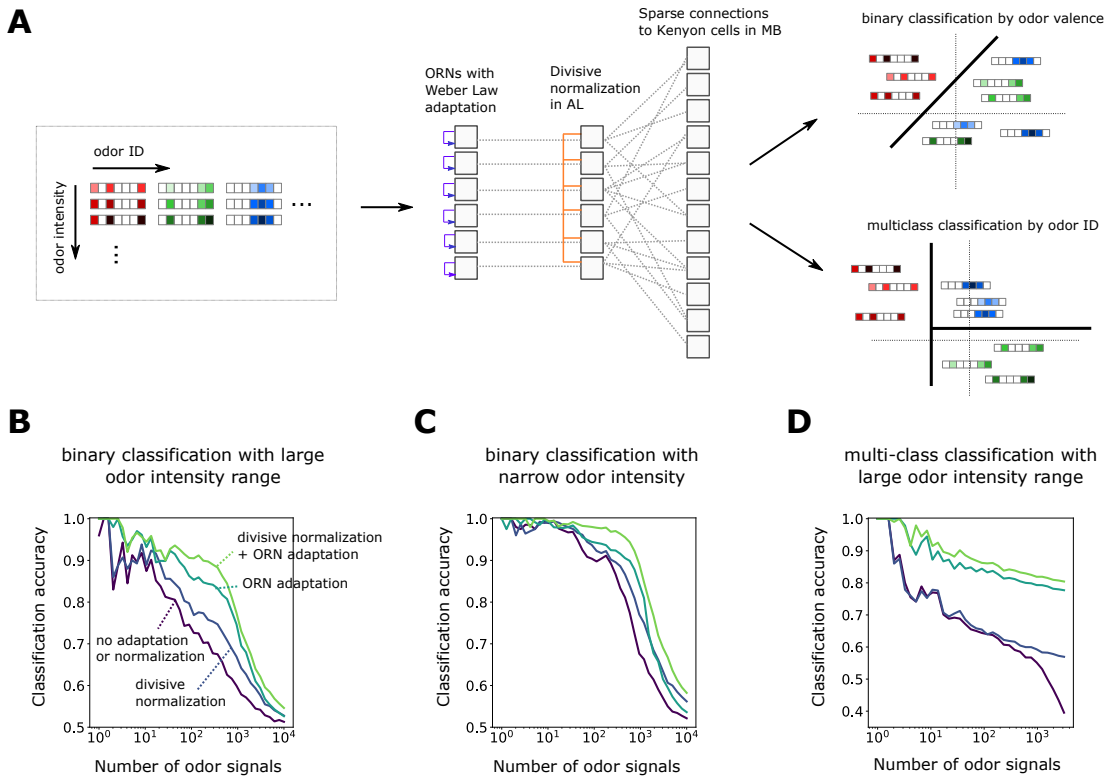

Figure 6: Dynamic adaptation maintains signal decoding fidelity amid fluctuating backgrounds at disparate timescales. **A** Traces of both odor signals, for three environments of increasingly faster background odor fluctuations. **B** Mis-identified odorants of foreground odor (blue trace in (A)), as a function of the relative complexity of the two odors and the adaptation rate.

sical model of bacterial chemotaxis [33], and is mathematically equivalent to a recently proposed competitive binding model for ORN response [34], where it was shown that inclusion of inhibitory responses increases coding capacity of a distributed system of ORNs. Regarding decoding, recent works have pointed to the importance of a distributed response in inferring high-dimensional sparse signals [28, 35, 36]. In this work, we place particular importance on the impact of intensity variations that typify odor signals in natural environments, finding that in both static and fluctuating odor landscapes, adaptive sensing at the receptor level play a central role in the simultaneous decoding of odor intensity and odor identity.

a Maintaining a distributed response

We showed that for static odor signals, a broadly sensing but non-adaptive system can accurately estimate odor identities, though only in a limited window of concentration. In living systems, adaptation maintains information transfer by ensuring that the sensory system stays in a regime of maximum sensitivity [37]. In compressed sensing, the fidelity of signal decoding relies also on the combinatorics of the sensor response [30, 29, 31]. Indeed, it has been noted that *diffusivity* in sensing – here incorporated through the dispersity of binding constants – underlies effective compression of high-dimensional sparse signals into a limited receptor space. Still, the nonlinearity of the steady state receptor response, Eq. **??**, can affect the distributions of ORN activity as odor concentration increases. Thus, in the context of combinatorial coding, the central benefit conferred by the Weber Law scaling is not merely preventing ORN activities from saturating, but their distributions from distorting.

Importantly, we find that the advantages of pre-

serving combinatorial response carry over to more complex odor environments, where multiple odors must be discriminated. The ability to recognize weak odors over strong backgrounds is particularly relevant to olfaction in nature, where signal conflicts are pervasive. Absent Weber Law scaling, odor signals are mis-identified in the presence of strong backgrounds, producing accurate estimations only beyond a minimum intensity; this minimum itself increases with odor complexity. Further, the system is largely incapable of estimating both odors accurately – true discrimination – except in limited concentration windows. In principle, the adaptive system might also be susceptible to signal conflicts: mathematically, the activity distributions are invariant only in the limit that all odorants are of equal strength (Eq), so the large deviations of the weaker odorant concentrations from this mean value could lead to sensitive distortions in the distribution of ORN activities. Nonetheless, we find that odors at least as strong as the background can be identified irrespective of odor complexities. Likewise discrimination accuracy is more robust, preserved over sizable concentration windows.

b The timescales of adaptation mechanisms

We find that in naturalistic, intermittent odor environments, dynamic adaptation can promote active perception of sparse odors throughout whiffs. In particular, adaptation timescales around 100 ms are sufficient in maintaining ongoing refinements of perceived odor identity, and that these refinements confer robust and accurate odor identification within a short time (<500 ms) following whiff onset. We also find that sufficiently rapid adaptation aids odor intensity coding, although these gains are not as stark. Finally, dynamic adaptation can promote the accurate detection of fluctuating odors within background environments whose intensity variations are sufficiently slow.

Several studies have implicated the importance of ORN temporal dynamics in odor encoding [38, 26, 39, 40, 18, 41, 42, 43]. In mammalian olfaction, recent studies raise the possibility that the few most sensitive ORs are solely responsible for coding odor identity, a so-called "primacy code" [26]; such a representation is concentration invariant, as higher intensities would recruit the response of other, less sensitive receptors, but still retain this particular subset. While our results implicate *all* ORNs, not just the most sensitive, in faithful odor encoding [28], there are a few reasons to believe these two viewpoints are not inconsistent (aside from anatomical differences between the mammalian and insect olfactory periphery [44]). First, combinatorial coding applies to the identification of complex mixtures, not single odorants as tested in [26]. Second, while many odors may be encoded by distributed activity patterns in ORNs and corresponding glomeruli, some odors relevant for innate behaviors such as mating and feeding may contain their own dedicated pathways; these latter odors may rely on strong, specialized responses [43, 45]. The presence of broad and narrowly tuned olfactory receptors in *Drosophila* suggests that both combinatorial and primacy coding play distinct, complementary roles in naturalistic odor sensing.

Online Methods

a Stochastic odor-receptor binding model

We model an odor as an N-dimensional vector $\mathbf{s} = \langle s_1, ..., s_N \rangle$, where $s_i > 0$ are the concentrations of individual volatile molecules (odorants) comprising the odor. In addition, we assume that the odors are sparse in the space of odorants, so only K components of $\mathbf{s}$ are nonzero, where $K \ll N$. The olfactory sensory system is modeled as a collection of M distinct Or/Orco complexes, each of which can be bound with any one of the odorant molecules, and can be either active (firing) inactive (quiescent). We only consider competitive binding, so a complex is bound with one odorant at most. With N possible odorants, receptor a resides in one of $2N + 2$ possible states, $\{R_a$, R_a^*, R_a-s_i, R_a^*-$s_i\}$, indicating receptors that are unbound/inactive, unbound/active, inactive/bound to odorant i, and active/bound to odorant i, respectively. Unless otherwise indicated, we set $N = 100$, $K = 7$, and $M = 50$ throughout.

In the mean-field limit, the binding dynamics of these $2N+2$ states are described by the master equations:

$$\frac{d[R_a\text{-}s_i]}{dt} = k_{ia}^{+} s_i [R_a] - k_{ia}^{-} [R_a\text{-}s_i] \tag{7}$$

$$\frac{d[R_a^*\text{-}s_i]}{dt} = k_{ia}^{*+} s_i [R_a^*] - k_{ia}^{*-} [R_a^*\text{-}s_i], \tag{8}$$

when receptor R_a is either inactive (Eq. 7) or active (Eq. 8). Further, transitions between inactive and

active states are described in the mean limit via:

$$\frac{d[R_a]}{dt} = w_a^{\mathrm{u}+}[R_a] - w_a^{\mathrm{u}-}[R_a^*] \tag{9}$$

$$\frac{d[R_a^*\text{-}s_i]}{dt} = w_{ia}^{\mathrm{b}+}[R_a\text{-}s_i] - w_{ia}^{\mathrm{b}-}[R_a^*\text{-}s_i], \tag{10}$$

when receptor R_a is either unbound (Eq. 9) or bound (Eq. 10). The corresponding disassociation constants in terms of the binding transition rates are:

$$K_{ia} = \frac{k_{ia}^-}{k_{ia}^+}$$
$$K_{ia}^* = \frac{k_{ia}^{*-}}{k_{ia}^{+*}} \tag{11}$$

Following [14], we assume that in steady state, the active firing state of an Or/Orco complex is energetically suppressed from the inactive state through corresponding Boltzmann factors:

$$\frac{[R_a^*]}{[R_a]} = \frac{w_a^{\mathrm{u}+}}{w_a^{\mathrm{u}-}} \equiv e^{-\epsilon_a} \tag{12}$$

$$\frac{[R_a^*\text{-}s_i]}{[R_a\text{-}s_i]} = \frac{w_{ia}^{\mathrm{b}+}}{w_{ia}^{\mathrm{b}-}} \equiv e^{-\epsilon_{ia}^{\mathrm{b}}}. \tag{13}$$

These energies are related through detailed balance, which we assume. Applying detailed balance to a given 4-cycle

$$R_a \to R_a^* \to R_a^*\text{-}s_i \to R_a\text{-}s_i \to R_a \tag{14}$$

gives

$$\frac{w_a^{\mathrm{u}+}}{w_a^{\mathrm{u}-}} \frac{k_{ia}^{*+}}{k_{ia}^{*-}} \frac{w_{ia}^{\mathrm{b}-}}{w_{ia}^{\mathrm{b}+}} \frac{k_{ia}^-}{k_{ia}^+} \equiv 1, \tag{15}$$

which, in conjunction with Eqs. 11, 12, and 13, gives

$$\epsilon_{ia}^{\mathrm{b}} = \epsilon_a + \ln\left[\frac{K_{ia}^*}{K_{ia}}\right]. \tag{16}$$

Assuming the binding dynamics are fast, then the probability that receptor a is bound by ligand i when inactive and active can be derived from Eqs. 7 and 8 as

$$p_{ia}^{\mathrm{b}} = \frac{s_i/K_{ia}}{1 + \sum_j^N s_j/K_{ja}} \tag{17}$$

$$p_{ia}^{\mathrm{b},*} = \frac{s_i/K_{ia}^*}{1 + \sum_j^N s_j/K_{ja}^*}. \tag{18}$$

The average activity A_a of complex a is the likelihood that the complex is active, unbound or unbound (equivalantly, the proportion of Or/Orco complexes in a given ORN that are active):

$$A_a = \frac{[R_a^*] + \sum_i^N [R_a^*\text{-}s_i]}{[R_a^*] + \sum_i^N [R_a^*\text{-}s_i] + [R_a] + \sum_i^N [R_a\text{-}s_i]}. \tag{19}$$

Using the master equations between active and inactive states Eq. 9 and 10, this activity obeys the master equation

$$\frac{dA_a}{dt} = w_a^+(1 - A_a) + w_a^- A_a \tag{20}$$

with effective transition rates

$$w_a^+ = \sum_i^N p_{ia}^{\mathrm{b}} w_{ia}^{\mathrm{u}+} + p_a w_a^{\mathrm{u}} \tag{21}$$

and analogously for w_a^-. Setting Eq. 20 to zero gives the steady state average activity level of ORN a:

$$A_a = \left(1 + e^{\epsilon_a} \frac{1 + \sum_i^N s_i/K_{ia}}{1 + \sum_i^N s_i/K_{ia}^*}\right)^{-1}. \tag{??}$$

b Generation of binding matrices K_{ia}^*

K_{ia}^* matrices are generated by sampling at two stages. First, for each receptor complex a, the disassociation constants for ligand i were chosen uniformly: $K_{ia}^* \sim \mathcal{U}[\mu_a, \nu_a]$. Each of these bounds were themselves drawn from a hyperdistribution, also uniform, $\mu_a \sim \mathcal{U}[\mu_{a,\mathrm{L}}, \mu_{a,\mathrm{H}}]$ and $\nu_a \sim \mathcal{U}[\nu_{a,\mathrm{L}}, \nu_{a,\mathrm{H}}]$. The hyperdistribution determines receptor diversity (which receptors are broadly versus narrowly tuned), while the target distribution for a given a determines that receptor's particular tuning curve. K_{ia} matrix elements were set identically to 1e3 throughout.

c Compressed sensing decoding of ORN response

We decode ORN responses to infer odor signal identities using an abstraction intended to mimic the neural computations underlying odor identification in the *Drosophila* mushroom body. While we make no assumptions that the compressed sensing (CS) algorithm (or one like it) is being utilized in actuality, this framework nonetheless informs our understanding of how the neural representation of odor identity is maintained or lost when passed through a distributed ORN repertoire. In this sense, CS is somewhat of an upper bound on how well a real neural

computation might perform in decompressing ORN responses.

We assume that ORN firing rates are linear in the Or/Orco complex activity; for simplicity we let this transform be the identity. Though subsequent neural circuitry, particularly from the glomeruli in the AL to the Kenyon cells in the MB further mix and scramble these responses, we focus here on the information transfer at the sensory periphery alone. In any case, as demonstrated previously [28], we expect that these neural computations would only improve the representation of neural identity, so we expect no negative ramifications for our findings.

CS addresses the problem of determining a sparse signal from a set of linear measurements, when the number of measurements is less than the signal dimension. Specifically, it is a solution to

$$\mathbf{y} = \mathbf{R}\mathbf{s}, \tag{22}$$

where $\mathbf{s} \in \mathbb{R}^N$ and $\mathbf{a} \in \mathbb{R}^M$ are vectors of signals and responses, respectively, and $\mathbf{R}$ is the measurement matrix. Since measurements are fewer than signal components, then $M < N$, whereby $\mathbf{R}$ is wide rectangular and so Eq. 22 cannot be simply inverted to produce $\mathbf{s}$. The idea of CS is to utilize the knowledge that $\mathbf{s}$ is sparse, i.e.g only K of its components, $K \ll N$ are nonzero. Both the measurements and sparsity are thus combined into a single constrained optimization routine:

$$\hat{s}_i = \text{argmin} \sum_i^N |s_i| \quad \text{such that } \mathbf{y} = \mathbf{R}\mathbf{s} \tag{23}$$

where $\hat{s}_i$ are the optimal estimates of the signal components and the sum, which is known as the L_1 norm of $\mathbf{s}$, is a natural metric of sparsity.

Importantly, the L_1 norm is a convex operation and the constraints are linear, so the optimization has a unique global minimum. To incorporate the nonlinear response of our encoding model into this linear framework, we assume that the responses are generated through the full nonlinear steady state response, Eq. **??**, but that the measurement matrix needed for decoding uses a linear approximation of this transformation. Expanding Eq. **??** around $s_0 = s_i - \Delta s_i$ gives

$$A_a \approx A_{a,0} + \Delta A_a \tag{24}$$

$$\Delta A_a = \sum_i^N R_{ia}\big|_{s_0} \Delta s_i \tag{25}$$

$$A_{a,0} = \frac{\sum_1^N s_0/K_{ia}^*}{\sum_1^N s_0/K_{ia}^* + e^{\epsilon_a}} \tag{26}$$

$$R_{ia}\big|_{s_0} = \frac{e^{\epsilon_a}/K_{ia}^*}{(\sum_i^N s_0/K_{ia}^* + e^{\epsilon_a})^2}, \tag{27}$$

where we work in the approximation $K_{ia}^* \ll s_0 \ll K_{ia}$. We assume that the neural system has access to the linearized response, Eq. 27, but must infer the excess signals Δs_i from the excess activity ΔA_a. Corresponding to the CS framework, therefore, $\Delta\mathbf{A} \to \mathbf{y}$, $\Delta\mathbf{s} \to \mathbf{s}$, and $R_{ia}\big|_{s_0} \to \mathbf{R}$. We optimize the cost function in Eq. 23 using sequential least squares programming, implemented in Python through using the scientific package SciPy.

d Or/Orco energies of activation ϵ_a and enforcement of Weber's Law

Free energies are considered receptor-independent throughout, with the exception of dynamically adaptive system in a temporal odor environment (Figs. 4 and **??**). To enforce Weber's Law, we assume the receptor activities feed back onto ϵ_a through the free energies. For the static case, adaptation is perfect, whereby Or/Orco activities are pegged to perfectly adapted values $\bar{A}_a$. Incorporating this into Eq. **??**, and assuming $K_{ia}^* \ll s \ll K_{ia}$, gives

$$\bar{\epsilon}_a = \ln\left(\frac{1-\bar{A}_a}{\bar{A}_a}\right) + \ln\left(\sum_i^N \frac{s_i}{K_{ia}^*}\right). \tag{28}$$

Assuming that the excess signals are small, $\Delta s_i < s_0$, this gives

$$\epsilon_a \approx \ln(s_0) + \epsilon_{a,0}, \tag{29}$$

where $\epsilon_{a,0}$ are receptor-dependent constants. In the static case, we choose these constants such that ϵ_a in both adaptive and non-adaptive systems are equivalent, equal to ϵ_L, at a given low concentration, $s_{0,\text{L}}$. Below this concentration, we assume adaptation is not in effect, so $\epsilon_a = \epsilon_\text{L}$.

It is important to note that while the linearized gain Eq. 27 utilized by the decoding algorithm appears to rely on ϵ_a, by the above argument ϵ_a can in principle be determined by firing rates alone. That is, ϵ_a is inferred in time through integration of Eq. **??**, which relies only on the current ORN activity.

Figure	N	M	K	$\mu_{a,\mathrm{L}}$	$\mu_{a,\mathrm{H}}$	$\nu_{a,\mathrm{L}}$	$\nu_{a,\mathrm{H}}$	$\epsilon_{a,0}$	ϵ_{L}	ϵ_{H}	$s_{0,\mathrm{L}}$	s_k	$s_{k,\mathrm{F}}$
1c	200	40	6	$2 \cdot 10^{-4}$	10^{-3}	10^{-2}	1.0	5.4	5.4	10	-	$\mathcal{N}\left(\frac{s_0}{5}, \frac{s_0}{15}\right)$	–
3a	100	50	7	0.5	0.5	0.8	0.8	5.4	3.1	10	10^{-1}	$\mathcal{N}\left(\frac{s_0}{3}, \frac{s_0}{15}\right)$	–
3b	100	50	7	0.5	0.6	0.6	0.9	5.4	3.1	10	10^{-1}	$\mathcal{N}\left(\frac{s_0}{3}, \frac{s_0}{15}\right)$	—
3c	100	50	7	0.5	0.6	0.6	0.9	5.4	3.1	10	10^{-1}	$\mathcal{N}\left(\frac{s_0}{3}, \frac{s_0}{15}\right)$	–
??-??	100	50	7	0.5	0.6	0.6	0.9	5.4	3.1	10	10^{-1}	$\mathcal{N}\left(\frac{s_0}{3}, \frac{s_0}{15}\right)$	$\mathcal{N}(1, \frac{1}{5})$
4	100	50	7	0.5	0.6	0.6	0.9	–	–	–	10^{-2}	$\mathcal{N}\left(\frac{s_0}{3}, \frac{s_0}{9}\right)$	–
??	100	50	7	0.5	0.6	0.6	0.9	–	–	–	10^{-2}	$\mathcal{N}\left(\frac{s_0}{3}, \frac{s_0}{9}\right)$	–

Table 1: Parameters for simulations in all of the figures.

e Odor signals

Odor signals $\mathbf{s}$ are N-dimensional vectors presumed sparse whereby only K components, s_k are nonzero, $K \ll N$. The magnitudes of the nonzero components s_k are denoted $s_0 + \Delta s_k$. Here, Δs_k is a random vector, while s_0 is both the center of linearization and, in the case of the adaptive system, the value dictating the strength of adaptive feedback $\epsilon_a \sim \ln\langle s_0 \rangle$.

All the signal intensities are in arbitrary units, as they can be scaled to any range by a corresponding shift in the scales of K_{ia} and K^*_{ia}.

f Dynamic adaptation

Dynamic adaptation is enforced through

$$\frac{d\epsilon_a(t)}{dt} = \frac{1}{\tau_a}\left[A_a - \bar{A}_a\right]. \qquad (??)$$

The perfectly adapted activity levels $\bar{A}_a$ are determined by evaluating Eq. **??** at a given odor intensity, $s_{0,\mathrm{L}}$, corresponding to a minimum stimulus at which adaptation takes effect. The decoding step is assumed instantaneous, so decoded odor identity $\hat{\mathbf{s}}$ is determined by the current value of ϵ_a (which, by virtue of Eq. **??**, is determined by ORN activity a short time prior).

For the simulations with two fluctuating odors (Figs. **??**), the traces shown correspond to the values of s_0 (in blue) and $s_{0,\mathrm{b}}$ (orange), where $s_{0,\mathrm{b}}$ is the baseline concentration of the background odor components, to which the excess signals $\Delta s_{k,\mathrm{b}}$ are added to set the individual odorant concentrations. We choose $\Delta s_{k,\mathrm{b}} \sim \mathcal{N}(s_{k,\mathrm{b}}/3, s_{k,\mathrm{b}}/9)$.

g Parameter values used in all figures

Parameter values for all of the plots are listed in Table 1.

References

[1] A. Couto, M. Alenius, and B. J. Dickson, "Molecular, anatomical, and functional organization of the drosophila olfactory system," *Current Biology*, vol. 15, no. 17, 2005.

[2] L. Buck and R. Axel, "A novel multigene family may encode odorant receptors: a molecular basis for odor recognition," *Cell*, vol. 65, no. 1, pp. 175–187, 1991.

[3] B. Malnic, J. Hirono, T. Sato, and L. B. Buck, "Combinatorial receptor codes for odors," *Cell*, vol. 96, no. 5, pp. 713–723, 1999.

[4] G. Wang, A. F. Carey, J. R. Carlson, and L. J. Zwiebel, "Molecular basis of odor coding in the malaria vector mosquito anopheles gambiae," *Proceedings of the National Academy of Sciences*, vol. 107, no. 9, pp. 4418–4423, 2010.

[5] J. G. Hildebrand and G. M. Shepherd, "Mechanisms of olfactory discrimination: converging evidence for common principles across phyla," *Annual review of neuroscience*, vol. 20, no. 1, pp. 595–631, 1997.

[6] E. Hallem and J. Carlson, "Coding of odors by a receptor repertoire," *Cell*, vol. 125, no. 1, pp. 143–160, 2006.

[7] M. de Bruyne, K. Foster, and J. R. Carlson, "Odor coding in the drosophila antenna," *Neuron*, vol. 30, no. 2, pp. 537 – 552, 2001.

[8] R. W. Friedrich and S. I. Korsching, "Combinatorial and chemotopic odorant coding in the zebrafish olfactory bulb visualized by optical imaging," *Neuron*, vol. 18, no. 5, pp. 737–752, 1997.

[9] R. I. Wilson, "Early olfactory processing in *Drosophila*: mechanisms and principles," *Annual Review of Neuroscience*, vol. 36, no. 1, pp. 217–241, 2013.

[10] J. Murlis, "Odor plumes and how insects use them," *Annual Review of Entymology*, vol. 37, pp. 505–532, 1992.

[11] M. Weissburg, "The fluid dynamical context of chemosensory behavior," *The Biological Bulletin*, vol. 198, no. 2, pp. 188–202, 2000. PMID: 10786940.

[12] A. Celani, E. Villermaux, and M. Vergassola, "Odor landscapes in turbulent environments," *Phys. Rev. X*, vol. 4, p. 041015, Oct 2014.

[13] R. T. Cardé and M. A. Willis, "Navigational strategies used by insects to find distant, windborne sources of odor," *Journal of Chemical Ecology*, vol. 34, pp. 854–866, Jul 2008.

[14] S. Gorur-Shandilya, M. Demir, J. Long, D. A. Clark, and T. Emonet, "Olfactory receptor neurons use gain control and complementary kinetics to encode intermittent odorant stimuli," *eLife*, vol. 6, p. e27670, jun 2017.

[15] "Olfactory signal coding in an odor background," *Biosystems*, vol. 136, pp. 35 – 45, 2015.

[16] G. Si, J. K. Kanwal, Y. Hu, C. J. Tabone, J. Baron, M. E. Berck, G. Vignoud, and A. D. Samuel, "Invariances in a combinatorial olfactory receptor code," *bioRxiv*, p. 208538, 2017.

[17] S. A. Montague, D. Mathew, and J. R. Carlson, "Similar odorants elicit different behavioral and physiological responses, some supersustained," *Journal of Neuroscience*, vol. 31, no. 21, pp. 7891–7899, 2011.

[18] C. Martelli, J. R. Carlson, and T. Emonet, "Intensity invariant dynamics and odor-specific latencies in olfactory receptor neuron response," *Journal of Neuroscience*, vol. 33, no. 15, pp. 6285–6297, 2013.

[19] S. R. Olsen, B. Vikas, and R. I. Wilson, "Divisive normalization in olfactory population codes," *Neuron*, vol. 66, pp. 287–299, 2010.

[20] M. Papadopoulou, S. Cassenaer, T. Nowotny, and G. Laurent, "Normalization for sparse encoding of odors by a wide-field interneuron," *Science*, vol. 332, no. 6030, pp. 721–725, 2011.

[21] E. H. Weber, *EH Weber on the tactile senses*. Psychology Press, 1996.

[22] J. Cafaro, "Multiple sites of adaptation lead to contrast encoding in the *Drosophila* olfactory system," *Physiological Reports*, vol. 4, no. 4, p. e12762, 2016.

[23] L.-H. Cao, B.-Y. Jing, D. Yang, X. Zeng, Y. Shen, Y. Tu, and D.-G. Luo, "Distinct signaling of *Drosophila* chemoreceptors in olfactory

sensory neurons," *Proceedings of the National Academy of Sciences*, vol. 113, no. 7, pp. E902–E911, 2016.

[24] H. Guo and D. P. Smith, "Odorant receptor desensitization in insects," *Journal of Experimental Neuroscience*, vol. 11, pp. 1–5, 2017.

[25] H. Guo, K. Kunwar, and D. Smith, "Odorant receptor sensitivity modulation in *Drosophila*," *The Journal of Neuroscience*, vol. 37, no. 39, pp. 9465–9473, 2017.

[26] C. D. Wilson, G. O. Serrano, A. A. Koulakov, and D. Rinberg, "A primacy code for odor identity," *Nature Communications*, vol. 8, no. 1, p. 1477, 2017.

[27] H. Giaffar, D. Rinberg, and A. A. Koulakov, "Primacy model and the evolution of the olfactory receptor repertoire," 2018.

[28] K. Krishnamurthy, A. M. Hermundstad, T. Mora, A. M. Walczak, and V. Balasubramanian, "Disorder and the neural representation of complex odors: smelling in the real world," *bioRxiv*, vol. doi:10.1101/160382, 2017.

[29] D. Donoho, "Compressed sensing," *IEEE Transactions on Information Theory*, vol. 52, no. 4, pp. 1289–1306, 2006.

[30] E. Candes, J. Romberg, and T. Tao, "Robust uncertainy principles: Exact signal reconstruction from highly incomplete frequency information," *IEEE Transactions on Information Theory*, vol. 52, no. 2, pp. 489–509, 2006.

[31] S. Ganguli and H. Sompolinsky, "Compressed sensing, sparsity, and dimensionality in neuronal information processing and data analysis," *Annual Review of Neuroscience*, vol. 35, no. 1, pp. 485–508, 2012.

[32] G. Lan, P. Sartori, S. Neumann, V. Sourjik, and Y. Tu, "The energy-speed-accuracy tradeoff in sensory adaptation," *Nature physics*, vol. 8, no. 5, pp. 422–428, 2012.

[33] Y. Tu, T. S. Shimizu, and H. C. Berg, "Modeling the chemotactic response of Escherichia coli to time-varying stimuli," *Proceedings of the National Academy of Sciences*, vol. 105, no. 39, pp. 14855–14860, 2008.

[34] L.-H. Cao, D. Yang, W. Wu, X. Zeng, B.-Y. Jing, M.-T. Li, S. Qin, C. Tang, Y. Tu, and D.-G. Luo, "Odor-evoked inhibition of olfactory sensory neurons drives olfactory perception in *Drosophila*," *Nature Communications*, vol. 8, no. 1, p. 1357, 2017.

[35] T. Tesileanu, S. Cocco, R. Monasson, and V. Balasubramanian, "Environmental adaptation of olfactory receptor distributions," *bioRxiv*, vol. doi:10.1101/255547, 2018.

[36] Y. Zhang and T. O. Sharpee, "A robust feedforward model of the olfactory system," *PLOS Computational Biology*, vol. 12, no. 4, pp. 1–15, 2016.

[37] I. Nemenman, "Information theory and adaptation," *arXiv*, vol. doi:[q-Bio]1011.5466, 2010.

[38] N. Gupta and M. Stopfer, "Insect olfactory coding and memory at multiple timescales," *Current Opinion in Neurobiology*, vol. 21, pp. 768–773, 2011.

[39] S. Junek, E. Kludt, F. Wolf, and D. Schild, "Olfactory coding with patterns of response latencies," *Neuron*, vol. 67, no. 5, pp. 872 – 884, 2010.

[40] C.-Y. Su, C. Martelli, T. Emonet, and J. R. Carlson, "Temporal coding of odor mixtures in an olfactory receptor neuron," *Proceedings of the National Academy of Sciences*, vol. 108, no. 12, pp. 5075–5080, 2011.

[41] D. W. Wesson, R. M. Carey, J. V. Verhagen, and M. Wachowiak, "Rapid encoding and perception of novel odors in the rat," *PLoS Biology*, vol. 6, p. e82, 2008.

[42] H. Sanders, B. E. Kolterman, R. Shusterman, D. Rinberg, A. Koulakov, and J. Lisman, "A network that performs brute-force conversion of a temporal sequence to a spatial pattern: relevance to odor recognition," *Frontiers in Computational Neuroscience*, vol. 8, p. 108, 2014.

[43] Y. Seki, H. K. Dweck, J. Rybak, D. Wicher, S. Sachse, and B. S. Hansson, "Olfactory coding from the periphery to higher brain centers in the drosophila brain," *BMC Biology*, vol. 15, p. 56, 2017.

[44] B. S. Hansson and M. C. Stensmyr, "Evolution of insect olfaction," *Neuron*, vol. 72, no. 5, pp. 698 – 711, 2011.

[45] M. N. Andersson, C. Lfstedt, and R. D. Newcomb, "Insect olfaction and the evolution of receptor tuning," *Frontiers in Ecology and Evolution*, vol. 3, p. 53, 2015.